Published in final edited form as:
Chem Commun (Camb). 2012 June 14; 48(47): 5835–5837. doi:10.1039/c2cc32149a.

Engineering of lipid-coated PLGA nanoparticles with a tunable payload of diagnostically active nanocrystals for medical imaging†

Aneta J. Mieszawska[a], **Anita Gianella**[a], **David P. Cormode**[a], **Yiming Zhao**[b], **Andries Meijerink**[b], **Robert Langer**[c], **Omid C. Farokhzad**[d], **Zahi A. Fayad**[a], and **Willem J. M. Mulder**[a,*]

[a]Translational and Molecular Imaging Institute and Imaging Science Laboratories, Mount Sinai School of Medicine, One Gustave L. Levy Place, New York, New York 10029, USA [b]Condensed Matter and Interfaces, Utrecht University, The Netherlands [c]Department of Chemical Engineering, Massachusetts Institute of Technology, Cambridge, MA, USA [d]Laboratory of Nanomedicine and Biomaterials, Department of Anesthesiology, Brigham & Women's Hospital, Boston, MA, USA

Abstract

Polylactic-*co*-glycolic acid (PLGA) based nanoparticles are biocompatible and biodegradable and therefore have been extensively investigated as therapeutic carriers. Here, we engineered diagnostically active PLGA nanoparticles that incorporate high payloads of nanocrystals into their core for tunable bioimaging features. We accomplished this through esterification reactions of PLGA to generate polymers modified with nanocrystals. The PLGA nanoparticles formed from modified PLGA polymers that were functionalized with either gold nanocrystals or quantum dots exhibited favorable features for computed tomography and optical imaging, respectively.

Clinical imaging modalities such as computed tomography (CT) and magnetic resonance imaging (MRI) are routinely used for disease diagnosis and evaluation of treatment efficacy. Molecular imaging is the specific detection of biological processes *in vivo*.[1a] It relies on generating functionalizable probes with high payloads of contrast generating materials, which is often accomplished using nanotechnology.[1b] Some of such systems were reported previously by our group.[1c–g] Inorganic nanocrystals, like gold or quantum dots (QDs), are frequently used as contrast agents for imaging in biological applications. Metallic gold nanocrystals (AuNCs) are electron dense and exhibit a high X-ray attenuation coefficient making them particularly suitable for CT applications.[2a,b] Semiconductor quantum dots (QDs) display a broadband absorption in the UV/VIS range and a narrow emission that can be tuned to near IR by varying the nanocrystal size and composition.[2c] Low photobleaching and high fluorescence quantum yield have resulted in their widespread use in optical imaging.[2d] Both, AuNCs and QDs, can be synthesized with a variety of capping ligands that render them soluble in either organic or aqueous media[2e,f] and allow functionalization with other molecules.[2g,h]

Polymeric nanoparticles such as poly(lactic-*co*-glycolic acid) (PLGA) with incorporated drugs have high therapeutic potential.[3a–c] Recently, lipid-coated PLGA nanoparticles have

†Electronic supplementary information (ESI) available: Detailed procedures for synthesis, cell culture, and imaging techniques. See DOI: 10.1039/c2cc32149a

willem.mulder@mssm.edu; Fax: +1 212 534 2683; Tel: +1 212 241 7717.

been synthesized that combine liposomal characteristics of long circulation half-life and polymeric biodegradability.[3d] The PLGA core is coated with soybean lecithin and further stabilized with 1,2-distearoyl-*sn*-glycero-3-phosphoethanolamine-*N*-methoxy (polyethylene glycol) 2000 (DSPE–PEG) to provide long circulation half-lives *in vivo*. Moreover, the inclusion of functional PEG groups allows for attachment of targeting moieties.[3d,e] There is a growing interest in 'theranostic' PLGA nanoparticles that, as well as therapeutics, also contain diagnostically active materials, like inorganic nanocrystals, to enable imaging guided therapy. Nevertheless, incorporation of controllable quantities of nanocrystals into PLGA nanoparticles remains challenging.

In this communication we describe a novel method to add diagnostic features to lipid-coated PLGA nanoparticles, through the integration of varying amounts of AuNCs and QDs into the nanoparticle core, for CT and optical imaging, respectively. To that end we used an elegant esterification reaction to conjugate AuNCs[4a] and CdSe core CdS–CdZnS–ZnS multi-layer shell QDs[4b] to PLGA polymers in a 1 to 1 stoichiometry prior to nanoparticle synthesis. To enhance nanocrystal payload, multiple esterifications can be performed. The procedure is outlined in Scheme 1 (see ESI[†] for full details). The COOH groups of 11-mercaptoundecanoic acid (MUA) ligands were reacted with OH groups of PLGA polymers or OH groups of 11-mercapto-1-undecanol (MUD) ligands were reacted with COOH groups of PLGA using dicyclohexylcarbodiimide mediated reaction with dimethyl-amino pyridine as a nucleophilic catalyst, which results in the formation of an ester bond between the ligands of nanocrystals and PLGA monomers. The same reaction was carried out to cross react AuNCs at the ends of PLGA with free AuNCs to form AuNC clusters for increased loading. PLGA polymers with chemically bound AuNCs and QDs were used to synthesize the lipid-coated PLGA nanoparticles *via* a nanoprecipitation method,[4c] rendering a hybrid nanoparticle that has a polyethylene glycol and soybean lecithin coating, a PLGA core, and a high payload of nanocrystals. Upon polymer degradation *in vivo*, the nanocrystals can be released, and their size range (1–10 nm) together with aqueous solubility enables their elimination through the urinary system.[4d]

Fig. 1 shows negative stain TEM images of lipid-PLGA nanoparticles with encapsulated AuNCs. Fig. 1A shows plain PLGA nanoparticles without nanocrystals incorporated. The mean diameter of these nanoparticles was 55.7 nm with a polydispersity of 0.116 as established by dynamic light scattering. Fig. 1B shows PLGA nanoparticles formed from polymer–AuNCs conjugates after one round of esterification reaction (PLGA–AuNCs–×1). The average diameter of nanoparticles was 65.5 nm with a polydispersity of 0.112. In these formulations 8 ± 3 AuNCs per PLGA nanoparticle were included (shown by arrow). In Fig. 1C PLGA nanoparticles formed from polymers that underwent two esterification reactions with AuNCs (PLGA–AuNCs–×2). This resulted in a dramatic increase in the number of AuNCs to 189 ± 73 per PLGA nanoparticle and appeared uniformly distributed throughout the nanoparticle core. The diameter of the PLGA–AuNCs–×2 increased to 98.4 nm with 0.118 polydispersity. The third repetition of the esterification reaction (PLGA–AuNCs–×3) led to a further increase of AuNCs to 829 ± 93 per PLGA nanoparticle (Fig. 1D) and an increased diameter of 116.6 nm with a 0.112 polydispersity. Although the size of PLGA–AuNC nanoparticles increases as gold loading increases, the diameter of ~100 nm is still within a favorable range for nanoparticles applied in biomedicine.[5a] The increase of AuNCs loading in the nanoparticles can be observed with the naked eye as a darkening of the red/brownish color of the nanoparticle solution (Fig. 1E). The CT contrast generated by AuNCs, encapsulated in PLGA nanoparticles, is shown in Fig. 1F. The calculated CT attenuation of AuNCs was 5.23 HU mM^{-1} and attenuation of commercially available iodine-based contrast

[†]Electronic supplementary information (ESI) available: Detailed procedures for synthesis, cell culture, and imaging techniques. See DOI: 10.1039/c2cc32149a

agent Isovue-370 (Bracco Diagnostics Inc., NJ, USA) was found to be 4.15 HU mM^{-1}. Similar findings were previously reported by Kim *et al.*[5b] where gold produced higher X-ray attenuation than an iodine contrast agent.

Fig. 2A depicts a negative stain TEM image of PLGA–QDs nanoparticles. The single esterification reaction between MUD capped QDs and PLGA polymers resulted in several QDs per PLGA nanoparticle. The sensitivity of optical imaging, which facilitates the detection of low QDs payloads, as well as fluorescence quenching by QD clustering[5c] made us decide not to perform multiple rounds of esterification. The absorbance and emission spectra of PLGA–QDs nanoparticles are shown in Fig. 2B. The peak for QDs is difficult to identify in the absorption spectrum since it shows strong scattering that increases towards shorter wavelengths, resulting from many constituents of the nanoparticle. However the absorption peak at 580–610 nm and the emission peak at 620 nm corresponding to QDs can be easily identified in the excitation and emission spectra, respectively. Also, the bright fluorescence can be observed by the naked eye using a hand held UV lamp (inset of Fig. 2B). The Cd-based QDs were used as model nanocrystals for optical applications. The low payload of QDs limits the potential cadmium related toxicity and if needed the QDs with an alternative and cadmium free composition can be used.

To demonstrate the capability of the nanoparticles to produce image contrast in a biological setting, we incubated the nanoparticles with mouse macrophage cells, type J774A.1. For PLGA–AuNCs nanoparticles cells were incubated at 0.25 mg of Au per ml of media, a corresponding concentration of Isovue, and with media only, collected as pellets after 4 hours, and imaged on a 256-slice Brilliance iCT scanner at 140 keV. The AuNCs produced CT contrast, detected as an increase in brightness, and cell pellets can be easily discerned, as shown in Fig. 3A (arrow). There is no CT contrast observed in pellets from media only or Isovue. The cell pellets with PLGA–QDs nanoparticles after 1 hour incubation were evaluated using an IVIS fluorescence imaging system. The cell pellet with PLGA–QDs shows strong fluorescence, while fluorescence was not detectable in cells incubated with media (Fig. 3B). Fig. 3C shows a TEM image of cells incubated with PLGA–AuNCs, with nanoparticles detected in the cell compartments. Fig. 3D shows a confocal image of cells after incubation with PLGA–QDs, showing bright red fluorescence in cells.

In summary, we have demonstrated a simple method to incorporate high payloads of AuNCs or QDs into PLGA nanoparticles through a ligand–polymer and ligand–ligand esterification reaction, to produce diagnostically active lipid-PLGA nanoparticles. The flexibility of the approach allows for multiple repetitions of the reaction to enhance the nanocrystal loading inside a PLGA core. The PLGA–AuNCs showed an X-ray attenuation superior to commercially used iodine-based contrast agents. The PLGA–QDs nanoparticles demonstrated bright fluorescence. The *in vitro* experiments confirmed the suitability of nanoparticles for biological and medical applications as image generating probes. This method can be extended to incorporate other nanocrystals, like iron oxide, silver or silica, into polymeric nanoparticles for imaging techniques or suitable biomedical applications.

Supplementary Material

Refer to Web version on PubMed Central for supplementary material.

Acknowledgments

This work was supported by the NHLBI, NIH, as a Program of Excellence in Nanotechnology (PEN) Award, Contract #HHSN268201000045C, R01 EB009638 (Z.A.F.), K99 EB012165 (D.P.C.) and R01 CA155432 (W.J.M.M.). This work was also supported by the Netherlands Organization for Scientific Research (NWO) ECHO. 06.B.047.

References

1. (a) Weissleder R, Mahmood U. Radiology. 2001; 219:316–333. [PubMed: 11323453] (b) Cho EC, Glaus C, Chen J, Welch MJ, Xia Y. Trends Mol. Med. 2010; 16:561–573. [PubMed: 21074494] (c) Gianella A, Jarzyna PA, Mani V, Ramachandran S, Calcagno C, Tang J, Kann B, Dijk WJ, Thijssen VL, Griffioen AW, Storm G, Fayad ZA, Mulder WJ. ACS Nano. 2011; 5:4422–4433. [PubMed: 21557611] (d) Jarzyna PA, Skajaa T, Gianella A, Cormode DP, Samber DD, Dickson SD, Chen W, Griffioen AW, Fayad ZA, Mulder WJ. Biomaterials. 2009; 30:6947–6954. [PubMed: 19783295] (e) Skajaa T, Zhao Y, van den Heuvel DJ, Gerritsen HC, Cormode DP, Koole R, van Schooneveld MM, Post JA, Fisher EA, Fayad ZA, de Mello Donega C, Meijerink A, Mulder WJ. Nano Lett. 2010; 10:5131–5138.(f) Cormode DP, Roessl E, Thran A, Skajaa T, Gordon RE, Schlomka JP, Fuster V, Fisher EA, Mulder WJ, Proksa R, Fayad ZA. Radiology. 2010; 256:774–782. [PubMed: 20668118] (g) Skajaa T, Cormode DP, Falk E, Mulder WJ, Fisher EA, Fayad ZA. Arterioscler., Thromb., Vasc. Biol. 2010; 30:169–176. [PubMed: 19815819]
2. (a) Hainfeld JF, Slatkin DN, Focella TM, Smilowitz HM. Br. J. Radiol. 2006; 79:248–253. [PubMed: 16498039] (b) Xu C, Tung GA, Sun S. Chem. Mater. 2008; 20:4167–4169. [PubMed: 19079760] (c) Dabbousi BO, Rodriguez-Viejo J, Mikulec FV, Heine JR, Mattoussi H, Ober R, Jensen KF, Bawendi MG. J. Phys. Chem. B. 1997; 101:9463–9475.(d) Michalet X, Pinaud FF, Bentolila LA, Tsay JM, Doose S, Li JJ, Sundaresan G, Wu AM, Gambhir SS, Weiss S. Science. 2005; 307:538–544. [PubMed: 15681376] (e) Templeton AC, Wuelfing WP, Murray RW. Acc. Chem. Res. 2000; 33:27–36. [PubMed: 10639073] (f) Selvan ST, Tan TT, Yi DK, Jana NR. Langmuir. 2010; 26:11631–11641. [PubMed: 19961213] (g) Hutter E, Maysinger D. Microsc. Res. Tech. 2011; 74:592–604. [PubMed: 20830812] (h) Larson DR, Zipfel WR, Williams RM, Clark SW, Bruchez MP, Wise FW, Webb WW. Science. 2003; 300:1434–1436. [PubMed: 12775841]
3. (a) Panyam J, Labhasetwar V. Adv. Drug Delivery Rev. 2003; 55:329–347.(b) Gu F, Langer R, Farokhzad OC. Methods Mol. Biol. 2009; 544:589–598. [PubMed: 19488725] (c) Dhar S, Gu FX, Langer R, Farokhzad OC, Lippard SJ. Proc. Natl. Acad. Sci. U. S. A. 2008; 105:17356–17361. [PubMed: 18978032] (d) Chan JM, Zhang L, Yuet KP, Liao G, Rhee JW, Langer R, Farokhzad OC. Biomaterials. 2009; 30:1627–1634. [PubMed: 19111339] (e) Valencia PM, Hanewich-Hollatz MH, Gao W, Karim F, Langer R, Karnik R, Farokhzad OC. Biomaterials. 2011; 32:6226–6233. [PubMed: 21658757]
4. (a) Brust M, Walker M, Bethell D, Schiffrin DJ, Whyman R. Chem. Soc. J. Chem. Commun. 1994:801–802.(b) Xie R, Kolb U, Li J, Basche T, Mews A. J. Am. Chem. Soc. 2005; 127:7480–7488. [PubMed: 15898798] (c) Barichello JM, Morishita M, Takayama K, Nagai T. Drug Dev. Ind. Pharm. 1999; 25:471–476. [PubMed: 10194602] (d) Choi HS, Liu W, Misra P, Tanaka E, Zimmer JP, Itty Ipe B, Bawendi MG, Frangioni JV. Nat. Biotechnol. 2007; 25:1165–1170. [PubMed: 17891134]
5. (a) Ai J, Biazar E, Jafarpour M, Montazeri M, Majdi A, Aminifard S, Zafari M, Akbari HR, Rad HG. Int. J. Nanomed. 2011; 6:1117–1127.(b) Kim D, Park S, Lee JH, Jeong YY, Jon S. J. Am. Chem. Soc. 2007; 129:7661–7665. [PubMed: 17530850] (c) Noh M, Kim T, Lee H, Kim CK, Joo SW, Lee K. Colloids Surf., A. 2010; 359:39–44.

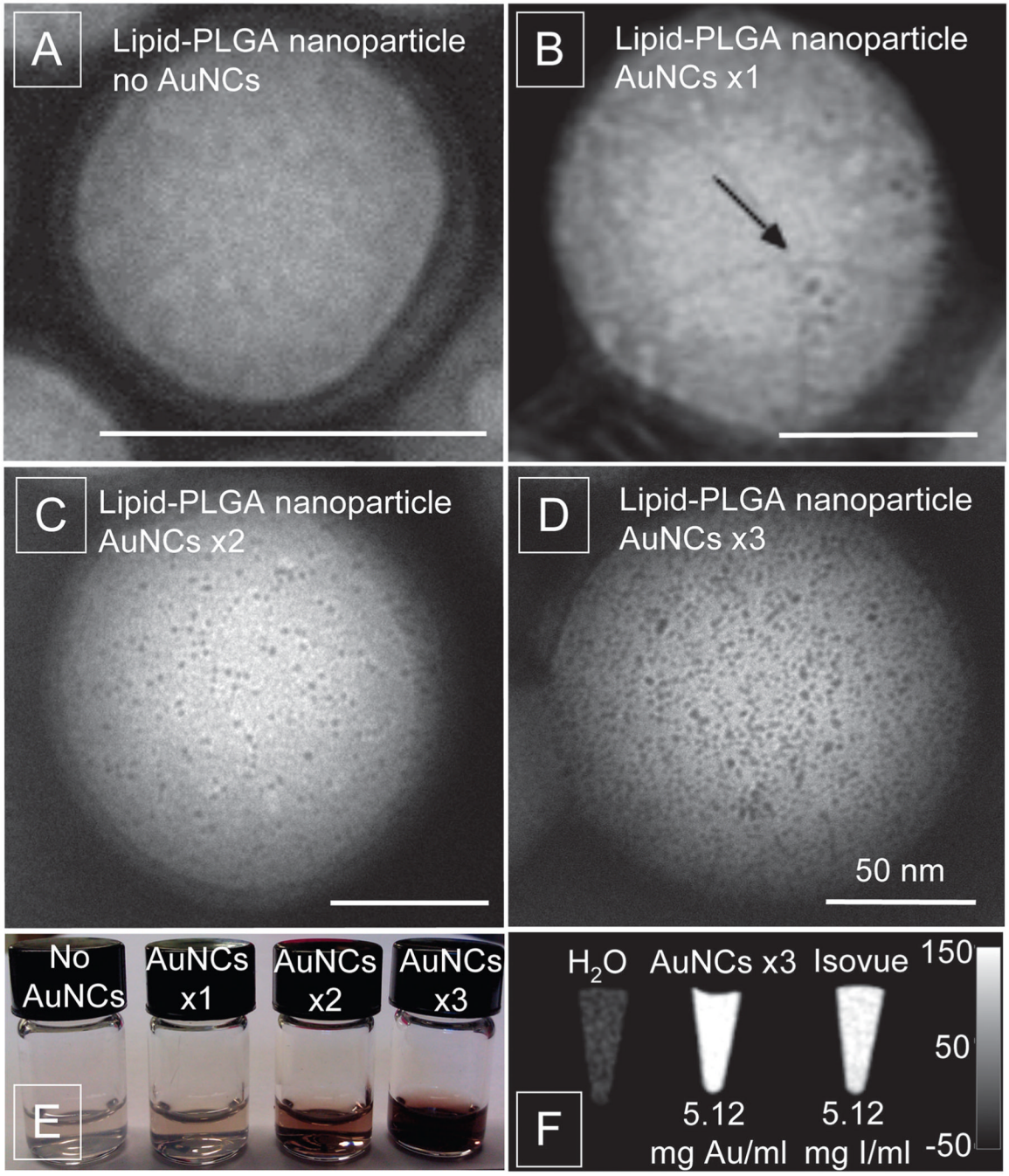

Fig. 1.

TEM images of lipid-PLGA nanoparticles only (A), and with AuNCs ×1 (B), AuNCs ×2 (C), and AuNCs ×3 (D); all scale bars are 50 nm. (E) Lipid-PLGA nanoparticles with increasing amounts of AuNCs. (F) CT contrast obtained from lipid-PLGA nanoparticles with AuNCs compared to Isovue and water at 140 kV and 250 mA (scale in Hounsfield units).

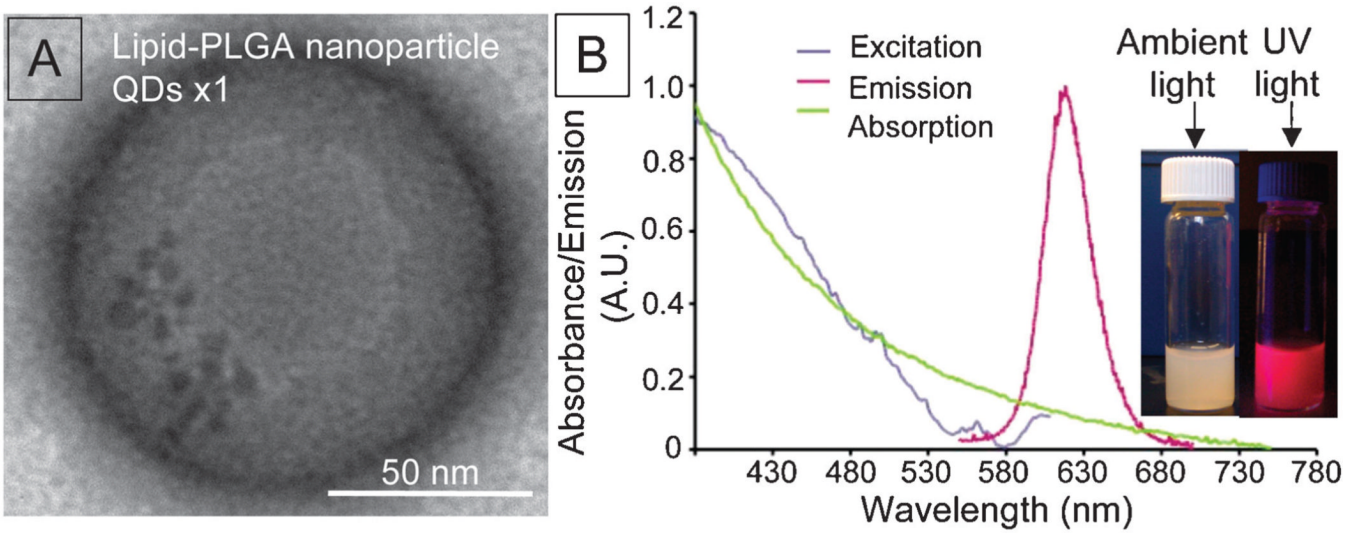

Fig. 2.
Lipid-PLGA nanoparticles with QDs (A) TEM image and (B) absorbance and emission spectra; inset: lipid-PLGA nanoparticles under ambient light and UV illumination.

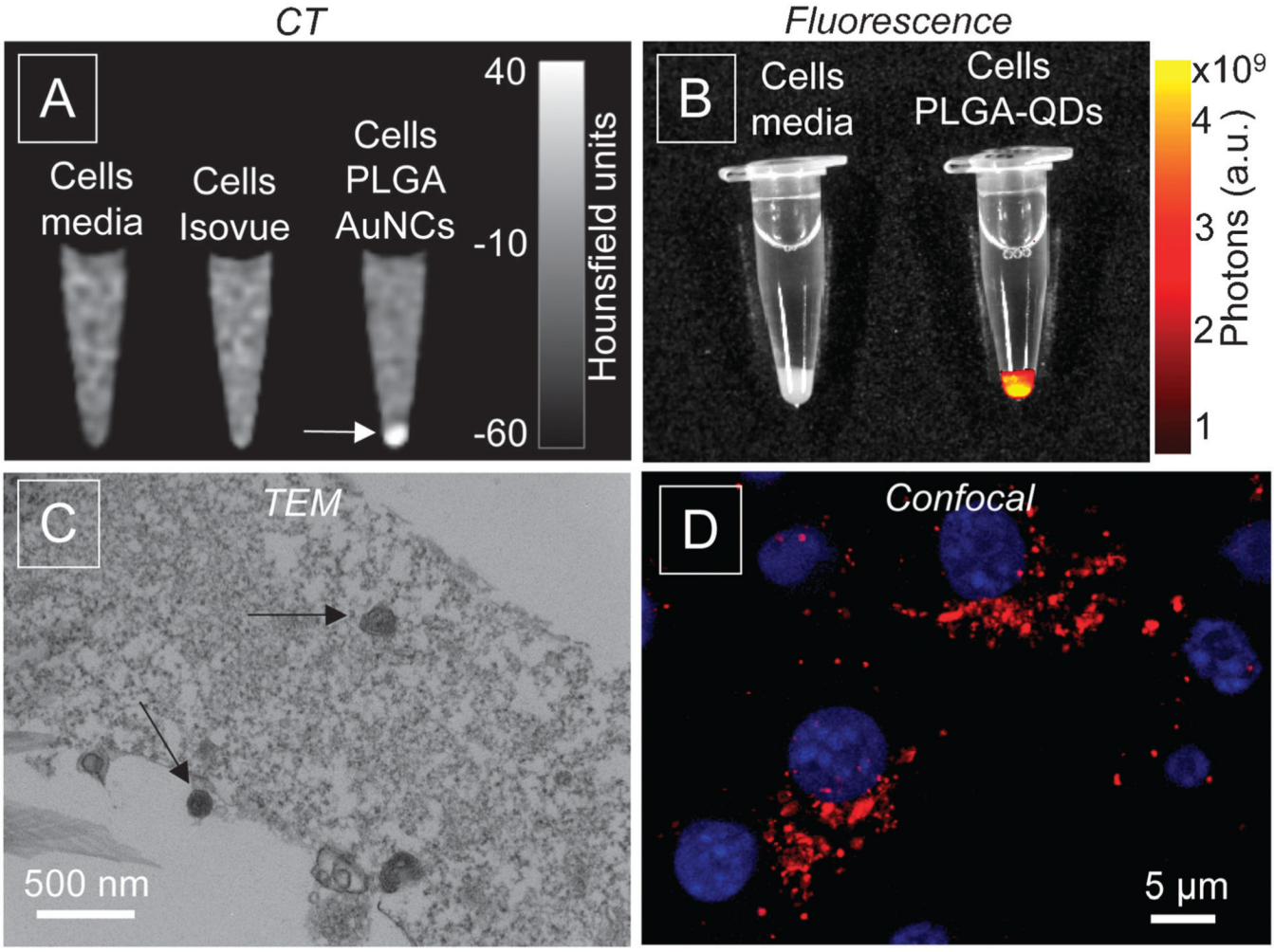

Fig. 3.

Results of *in vitro* experiments. (A) CT image and (B) fluorescent image of cell pellets, (C) TEM image of cells incubated with lipid-PLGA–AuNCs nanoparticles (arrows) and (D) confocal image of cells (nuclei in blue) incubated with lipid-PLGA–QDs nanoparticles (red).

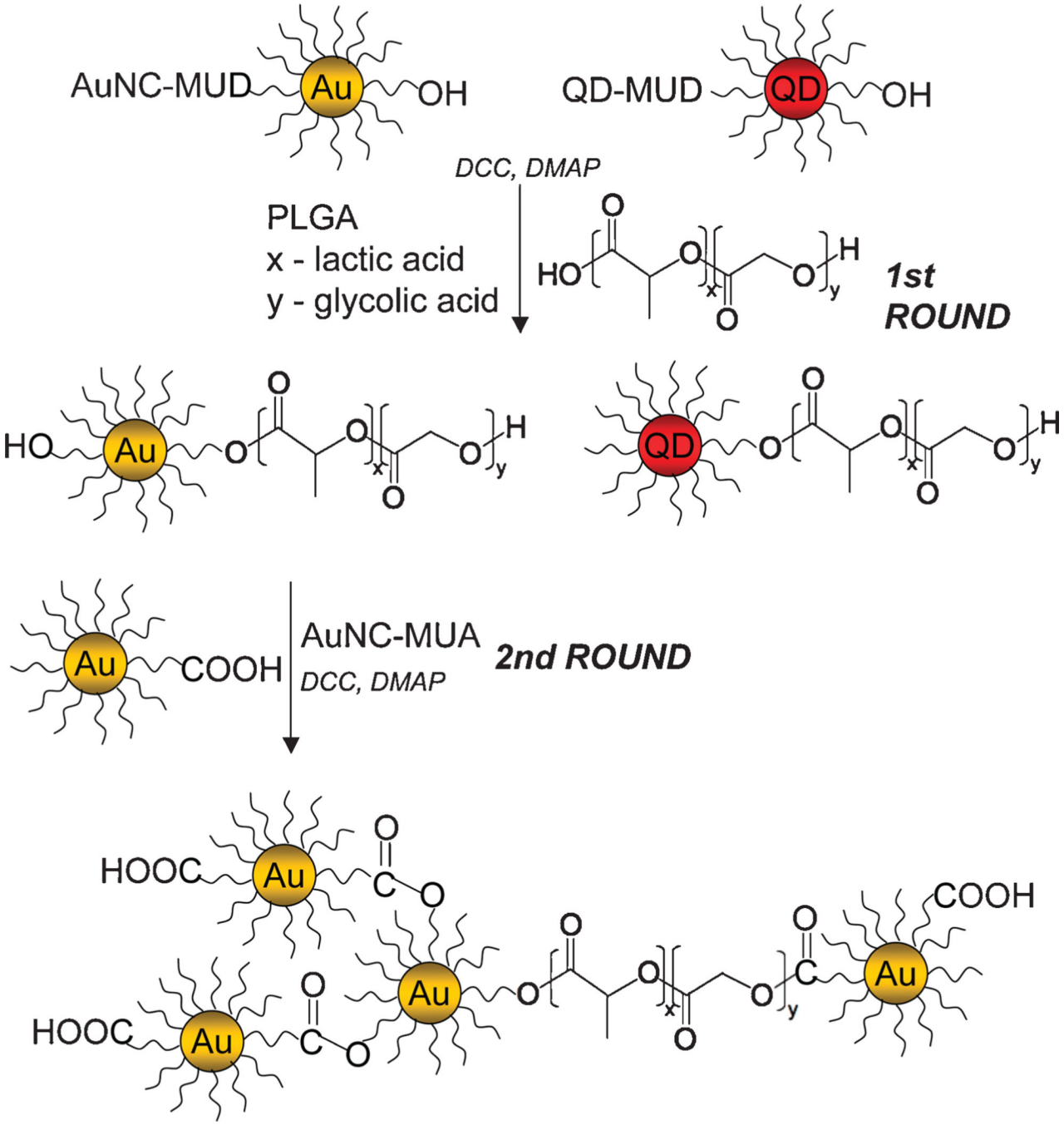

Scheme 1.
Procedure for chemical modification of PLGA polymers with nanocrystals.